J. Fluid Mech. (1977), *vol.* 80, *part* 1, *pp.* 153–177
Printed in Great Britain

Response of a turbulent boundary layer to a step change in surface heat flux

By R. A. ANTONIA,
Department of Mechanical Engineering, University of Newcastle, New South Wales 2308, Australia

H. Q. DANH
Department of Mechanical Engineering, University of Sydney, New South Wales 2006, Australia

AND A. PRABHU
Department of Aeronautics, Indian Institute of Science, Bangalore 560012

(Received 26 June 1975 and in revised form 27 May 1976)

Measurements of both the velocity and the temperature field have been made in the thermal layer that grows inside a turbulent boundary layer which is subjected to a small step change in surface heat flux. Upstream of the step, the wall heat flux is zero and the velocity boundary layer is nearly self-preserving. The thermal-layer measurements are discussed in the context of a self-preserving analysis for the temperature disturbance which grows underneath a thick external turbulent boundary layer. A logarithmic mean temperature profile is established downstream of the step but the budget for the mean-square temperature fluctuations shows that, in the inner region of the thermal layer, the production and dissipation of temperature fluctuations are not quite equal at the furthest downstream measurement station. The measurements for both the mean and the fluctuating temperature field indicate that the relaxation distance for the thermal layer is quite large, of the order of $1000\theta_0$, where θ_0 is the momentum thickness of the boundary layer at the step. Statistics of the thermal-layer interface and conditionally sampled measurements with respect to this interface are presented. Measurements of the temperature intermittency factor indicate that the interface is normally distributed with respect to its mean position. Near the step, the passive heat contaminant acts as an effective marker of the organized turbulence structure that has been observed in the wall region of a boundary layer. Accordingly, conditional averages of Reynolds stresses and heat fluxes measured in the heated part of the flow are considerably larger than the conventional averages when the temperature intermittency factor is small.

1. Introduction

The response of a turbulent boundary layer to a step change in surface conditions has received special attention both experimentally and theoretically, mainly because of its relevance to the atmospheric situation. Townsend (1965*a*, *b*)

considered the cases of a step change in surface roughness, a step change in surface heat flux or a combination of both. His assumption that the perturbation to the flow field caused by the change in boundary conditions is self-preserving in nature leads to a description of flow parameters such as the growth rate of the perturbed region or 'internal' layer and the surface shear stress and/or heat flux that is in reasonable agreement with the available atmospheric measurements.

Although a step change in surface roughness has been investigated experimentally in the laboratory in detail by several workers (for references see Antonia & Luxton 1971), few systematic investigations of a step in surface heat flux or surface temperature have appeared in the literature. Johnson (1957, 1959), Blom (1970) and Fulachier (1972) have all considered a step in surface temperature, although Fulachier's investigation was mainly concerned with a detailed study of the turbulence structure when the velocity and thermal layers have effectively the same origin. Interesting features of the above investigations are the observed temperature intermittency (Johnson) of the internal layer and relatively slow adjustment of temperature fluctuation intensity and enthalpy flux, mainly evident in Fulachier's measurements. Blom (1970) found that, for the developing layer, the turbulent Prandtl number Pr_t varied both across the layer and in the streamwise direction except in the near vicinity of the wall, where the increase in Pr_t with increasing distance from the wall was the same at all streamwise stations.

In this paper, we examine the development of a thermal layer downstream of a step change in surface heat flux and present measurements of several characteristics of the sharp thermal-layer interface. At the step, the zero-pressure-gradient turbulent boundary layer is fully developed. Results for the mean and fluctuating temperature fields are presented in §§4 and 5 and are, whenever possible, compared with the results for a fully developed layer of Fulachier. The measured growth of the thermal layer is compared in §4 with the predicted variation obtained from Townsend's (1965*a*) self-preservation analysis, which is reviewed briefly in §3. The passive temperature contaminant provides a simple means of studying the thermal interface, and in §6 use is made of the conditional sampling technique to obtain conditional averages of both temperature and velocity fluctuations both within and outside this interface.

2. Experimental arrangement and conditions

The contraction and working section of the wind tunnel used for the present investigation are the same as those described by Swenson (1973). The present wind tunnel has, however, a new centrifugal blower with a blower speed of about 2500 r.p.m. driven by a 8·4 kW Siemens motor with a Siemens thyristor speed controller; this allows a maximum speed in the working section of about 37 m s^{-1}. A new diffuser, built in two sections, and a settling chamber have also been provided. The working section is 38 cm wide and 23 cm high at the end of the contraction, the height of the roof being adjusted to achieve a zero pressure gradient for the present experimental conditions. The length of the working section is 4·9 m and the first 2 m of the floor consists of a Sindanyo hard asbestos board with an epoxy coating sanded to a smooth flat surface. The remainder

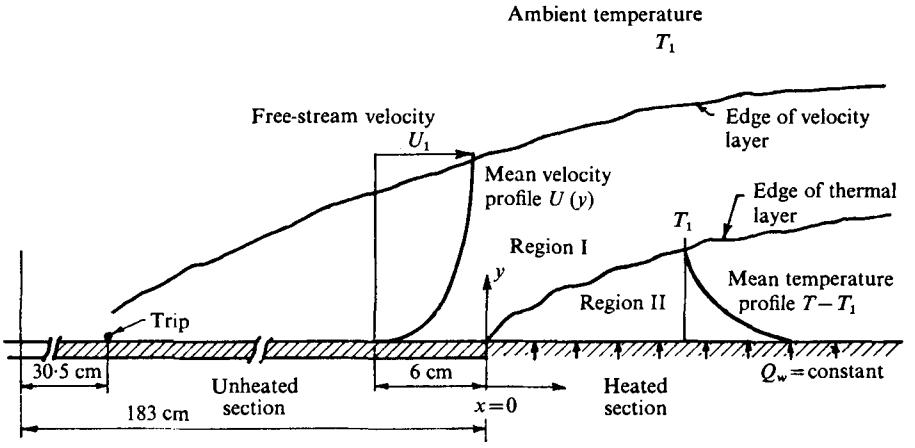

FIGURE 1. Schematic diagram of experimental situation.

of the floor consists of a heated plate, designed by Swenson (1973) and described in detail in his thesis. This heated section is made up of five identical plates each 61 cm long. Each plate has a Sindanyo base and four spanwise strips of Inconel (0·046 × 15·24 × 38·1 cm) bonded to this base with epoxy resin. The strips are electrically insulated from each other by epoxy-filled gaps ($\sim$ 0·038 cm wide) and the sides of the plates overhang the asbestos base and are soft-soldered to brass bus-bars. In the present work, the first four plates (i.e. 16 Inconel strips) were all connected in series to provide a reasonably constant distribution of wall heat flux over the 2·4 m heated section (the last plate was not heated). A.c. heating was used (60 A, 60 V) and it was found that only about 30 min of tunnel running time were needed to achieve steady-state heating conditions. The heated floor section was fitted with copper–constantan thermocouples consisting of wires of two sizes: those leading into the plate were 0·010 cm in diameter, were silver soldered at the hot junction and were jointed to thicker wire (0·030 cm diameter) at about 15 cm from the plate. The hot junctions were soft soldered into the plate whilst the cold junctions were kept at the ambient temperature of the laboratory in which the tunnel was situated. The laboratory was air conditioned and the ambient air temperature was maintained to within 1 % of the selected temperature ($\sim$ 26 °C for the present experiments). The thermocouples are situated at a number of stations in both the streamwise and the spanwise direction. The thermocouple e.m.f. was measured with a Cambridge portable potentiometer 44226 to a resolution of less than 10 μV.

The nominal free-stream velocity U_1 was 9·45 m s^{-1} and the boundary-layer thickness δ_0 (defined as the 0·995U_1 point) at the upstream edge of the heated section was 4·5 cm. The Reynolds number at that position was $R_{\theta_0} \simeq 3070$, where $R_{\theta_0} = U_1\theta_0/\nu$, θ_0 being the momentum thickness at $x = 0$ (figure 1).

Velocity (u horizontal, and v vertical) and temperature (θ) fluctuations were measured with a three-wire probe made up of a miniature DISA X-probe and a single wire sensitive only to θ. The X-probe consisted of platinum-coated tungsten wires 5 μm in diameter operated by two channels of DISA 55M01

constant-temperature anemometers. The 1 μm diameter platinum single 'cold' wire was operated by a constant-current anemometer (Stellema, Antonia & Prabhu 1975), with the value of the current set at 100 μA. All three wires were approximately 1 mm in length and the cold wire was mounted to one side of the X-probe in a direction normal to the wall and parallel to the plane of the X-probe.† The sensitivity coefficients of the X-wire were determined from a speed and yaw calibration in the isothermal external stream and from an assumed heat balance equation for the X-wire as given in Antonia, Prabhu & Stephenson (1975). The temperature contamination of the X-wire signals was removed by processing them on an EAI-180 analog computer (for details, see Antonia *et al.* 1975). Signals directly proportional to u, v and θ were then recorded on a Philips Analog 7 FM tape recorder at a speed of 38·1 cm s^{-1}. Records on tape were typically of duration 70–90 s. Root-mean-square values of u, v and θ were obtained by using either DISA 55D-35 r.m.s. meters or multipliers for squaring the signals and subsequently averaging the outputs on either a P.A.R. boxcar integrator, model CW-1, or a DISA true integrator, type 52B30.

The mean temperature profile in the thermal layer was obtained with a single (1 μm diameter) platinum cold wire arranged parallel to the wall and perpendicular to the flow direction. The temperature coefficient of resistivity of the platinum wire was found to be 0·0034 °C^{-1} ($\pm$ 3 %) by calibrating the wire against a copper–constantan thermocouple in the potential core of a jet (7·2 cm diameter nozzle) heated over a temperature range of about 20 °C above ambient room temperature. For measurements in the boundary layer, the d.c. output from the anemometer bridge was first adjusted to zero when the wire was in the tunnel free stream (ambient temperature T_1) so that the d.c. output when the wire was inside the thermal layer was directly proportional to the temperature difference $T - T_1$. For the wire used, the voltage/temperature sensitivity was 3·74 V/°C.

3. Self-preservation considerations

Before discussing the experimental results in detail, it is useful to consider the possibility of self-preserving development of the thermal layer which grows downstream of the step (figure 1). Here the thermometric wall heat flux Q_w is sufficiently small that the effect of density variations on the motion can be neglected. Following Townsend (1965), the mean temperature perturbation is assumed to be self-preserving, i.e.

$$T - T_1 = -\frac{\theta_0}{\kappa_\theta}\phi\left(\frac{y}{l_0}\right). \tag{1}$$

Here the temperature scale θ_0 and the length scale l_0 (representing the extent of the thermal layer) are assumed to depend on x only and the change in the mean temperature caused by a possible displacement of the mean streamline as it

† Another three-wire arrangement was used, whereby the cold wire was mounted on a sleeve which could slide over the stem of the X-probe. In this configuration the cold wire was kept horizontal and approximately 1 mm upstream of the X-wire intersection. The results obtained with this probe were in good agreement with those obtained with the first probe arrangement.

passes from region 1 into region 2 (figure 1) has been neglected. In region 2, the inner boundary conditions on T and the mean velocity U are given by the logarithmic relations

$$\frac{T_w - T}{\theta_\tau} = \frac{1}{\kappa_\theta} \ln \frac{yU_\tau}{\nu} + C_\theta \tag{2}$$

and

$$\frac{U}{U_\tau} = \frac{1}{\kappa} \ln \frac{yU_\tau}{\nu} + C \tag{3}$$

respectively, provided that the flow is in equilibrium. T_w is the wall temperature, U_τ is the friction velocity ($= \tau_w^{\frac{1}{2}}$, where τ_w is the kinematic wall shear stress) and θ_τ is the analogous friction temperature ($= Q_w/U_\tau$). C and C_θ are constants while κ_θ is, for this analysis, assumed equal to the Kármán constant κ ($= 0{\cdot}41$), an assumption that implies $Pr_t = 1$.

For small η ($= y/l_0$), $\phi \propto \ln \eta$ and θ_0 can be identified with θ_τ. Extending the concept of self-preservation to the turbulent heat flux $\overline{v\theta}$, we can write

$$\overline{v\theta} = Q_w \phi_1(\eta). \tag{4}$$

Substitution of (1) and (4) into the mean enthalpy equation

$$U \frac{\partial T}{\partial x} + V \frac{\partial T}{\partial y} + \frac{\partial \overline{v\theta}}{\partial y} = 0 \tag{5}$$

leads to the following requirements (to order $(l_0/z_0)^{-1}$, which is small) for self-preservation:

$$\frac{dl_0}{dx} \ln \frac{l_0}{z_0} \quad 2\kappa^2, \quad Q_w \propto l_0^n \tag{6a,b}$$

where z_0 ($= \nu e^{-C} \kappa / U_\tau$) is the 'roughness' length. In the present experiment n is equal to zero. To derive an explicit mean temperature distribution, Townsend (1965) uses the relation for the thermal mixing length l_θ:

$$\overline{v\theta} = l_\theta (-\overline{uv})^{\frac{1}{2}} \frac{\partial T}{\partial y}, \tag{7}$$

or, with $l_\theta = \kappa y$ for $Pr_t = 1$,

$$\phi_1 = \eta \phi.$$

The solution of (5) can be written as

$$\phi_1 = e^{-2\eta} \quad \text{or} \quad \phi = \mathrm{Ei}(-2\eta). \tag{8}$$

It should be emphasized that these self-preserving solutions are appplicable only when $l_0 \ll \delta$, $l_0 \gg z_0$ and provided thermal equilibrium is satisfied in the region near the wall. The relevance of these conditions and solutions to the present flow will be considered in the following sections.

4. Results for mean temperature field

The wall heat flux Q_w, shown in figure 2, is approximately constant over the range of x considered. The values of Q_w were obtained from the slopes of the approximately linear mean temperature profiles (see figure 3) obtained close to

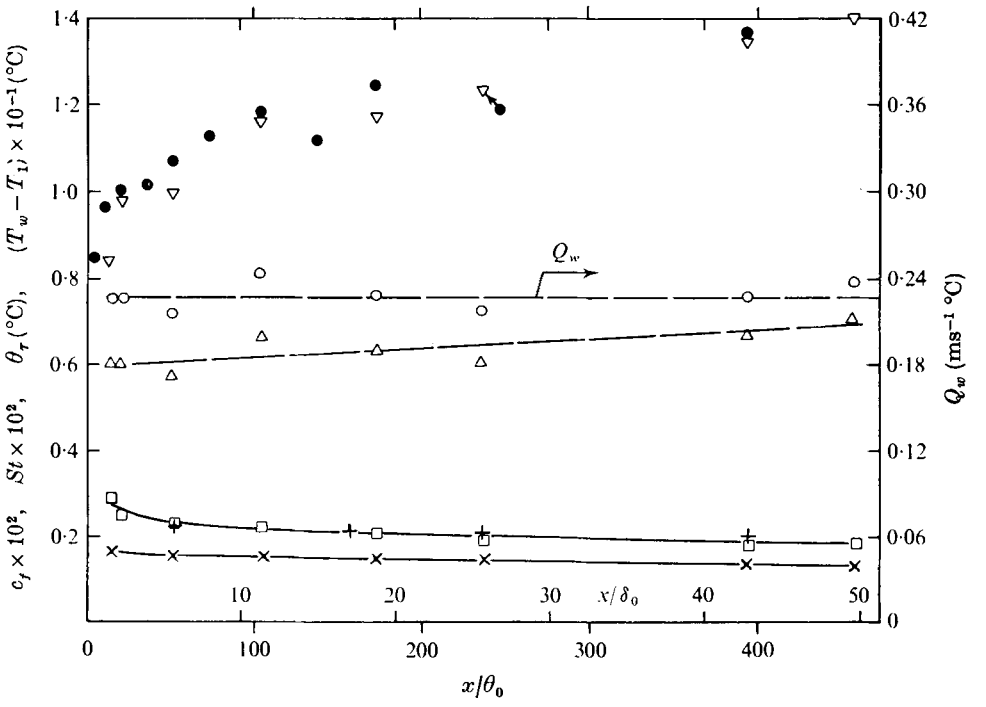

FIGURE 2. Variation of wall temperature, heat flux, friction velocity and friction temperature. ●, wall temperature defect $T_w - T_1$ (°C); ○, thermometric wall heat flux Q_w (m s^{-1} °C); △, friction temperature θ_τ(°C); □, Stanton number St; ×, skin friction $\frac{1}{2}c_f$.

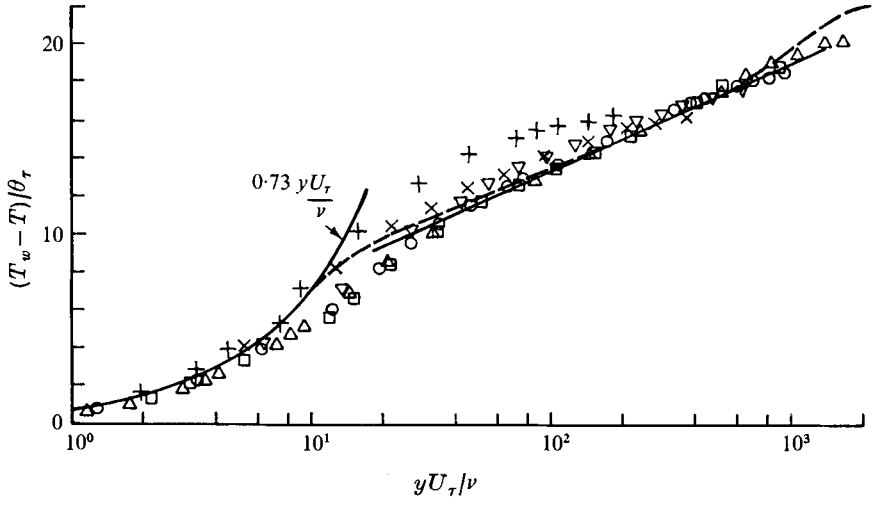

FIGURE 3. Mean temperature profiles in semi-logarithmic co-ordinates. +, $x/\delta_0 = 2{\cdot}3$; ×, $x/\delta_0 = 5{\cdot}7$; ▽, $x/\delta_0 = 11{\cdot}4$; ○, $x/\delta_0 = 18{\cdot}9$; □, $x/\delta_0 = 25{\cdot}7$; △, $x/\delta_0 = 42{\cdot}9$; —·—, linear region, $(T_w - T)/\theta_\tau = 0{\cdot}73yU_\tau/\nu$; ——, logarithmic region $(T_w - T)/\theta_\tau = 2{\cdot}4 \ln yU/\nu + 2{\cdot}0$; — —, Fulachier (1972), fully developed mean temperature profile.

the wall. Values of the wall temperature T_w inferred by extrapolating these profiles to the wall are in reasonable agreement with the surface thermocouple values.

The Stanton number St $(= Q_w/U_1[T_w - T_1])$, proportional to $T_w - T_1$ in this case, is appreciably larger in magnitude than $\frac{1}{2}c_f$ ($c_f = \tau_w/\frac{1}{2}U_1^2$ is the skin-friction coefficient determined from the measured mean velocity profiles by the Clauser method). This departure from unity of the ratio $St/\frac{1}{2}c_f$ (the Reynolds analogy factor) is however reasonably predicted by the calculation of Kays (1966, p. 244), corresponding to a step in wall heat flux at $U_1\theta_0/\nu \simeq 3000$. It should be noted here that the value of Q_w determined from the mean enthalpy integral relation

$$Q_w = d[(T_w - T_1)\,\delta_H]/dx, \quad \text{where} \quad \delta_H = \int_0^\infty \frac{U}{U_1}\left(\frac{T - T_1}{T_w - T_1}\right) dy$$

is the enthalpy thickness, is approximately 20% higher than that shown in figure 2. Also, the momentum-integral values of c_f $(= 2d\theta/dx)$ are about 25% higher than those shown in figure 2, implying a slight convergence of the mean-flow streamlines.†

The difference between the wall temperature T_w and the local temperature T is plotted in figure 3 with the use of the temperature scale θ_τ and length scale ν/U_τ. In the region near the wall $(yU_\tau/\nu < 8)$ the viscous-sublayer relation $(T_w - T)/\theta_\tau = 0{\cdot}73yU_\tau/\nu$, where 0·73 is the molecular Prandtl number, is a good fit to the data. For $x/\delta_0 = 2{\cdot}3$, there is little evidence of a linear region in the semi-log plot of figure 3. Although a linear region seems to be present at $x/\delta_0 = 5{\cdot}7$ and 11·4, the position of this region on the plot is higher than for the profiles at larger x/δ_0. A reasonable fit to the linear region for the profiles at $x/\delta_0 \geqslant 18{\cdot}9$ is given by the solid line [equation (2)] in figure 3 with $\kappa_\theta \simeq \kappa\,(= 0{\cdot}41)$ and $C_\theta = 2{\cdot}0$.

In the experiments of Fulachier (1972) (fully developed thermal layer with a constant wall temperature) and Bradshaw & Ferriss (1968) (step change in wall heat flux) κ_θ was found to be equal to 0·45. This discrepancy appears to be consistent with the values of the Prandtl number presented in § 5. The present value of C_θ (which is in general a function of the molecular Prandtl number and/or the pressure gradient) is lower than those of Fulachier (3·13), Bradshaw & Ferriss (3·33) and Blom (2·8). Note that the results in figure 3 could be interpreted to indicate a decrease in C_θ with increasing x in the early stages of development of the thermal layer.

In the outer part of the thermal layer, the mean temperature profiles deviate only slightly (figure 3) from the logarithmic relation. Even at $x/\delta_0 = 42{\cdot}9$, the deviation is significantly smaller than that obtained by Fulachier, indicating that a fully developed profile has not yet been established in the outer region of the thermal layer. The slow development of the mean temperature profile is also in evidence in figure 4, where $y = \delta_T$, defined as the point where $T - T_1 = 0{\cdot}01(T_w - T_1)$, is arbitrarily used to denote the outer edge of the thermal layer.

† The origin for this convergence was estimated to be approximately 15 m downstream of the start of the heated floor section.

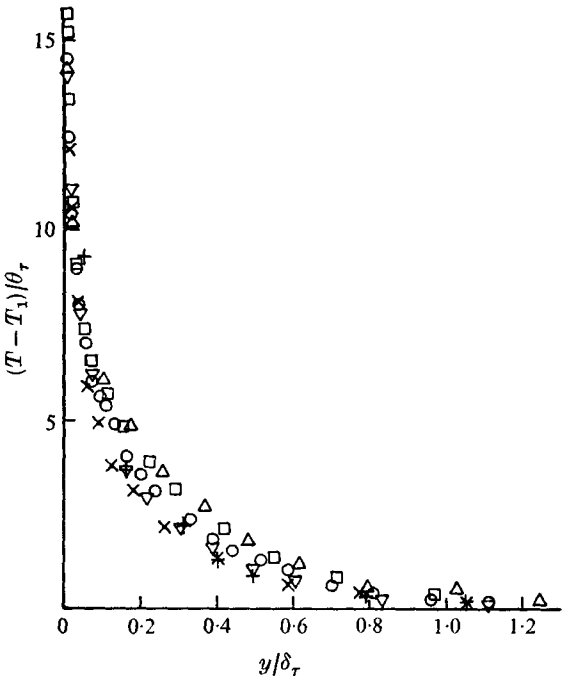

FIGURE 4. Mean temperature profiles as a function of y/δ_T. +, $x/\delta_0 = 2{\cdot}3$; ×, $x/\delta_0 = 5{\cdot}7$; ▽, $x/\delta_0 = 11{\cdot}4$; ○, $x/\delta_0 = 18{\cdot}9$; □, $x/\delta_0 = 25{\cdot}7$; △, $x/\delta_0 = 42{\cdot}9$.

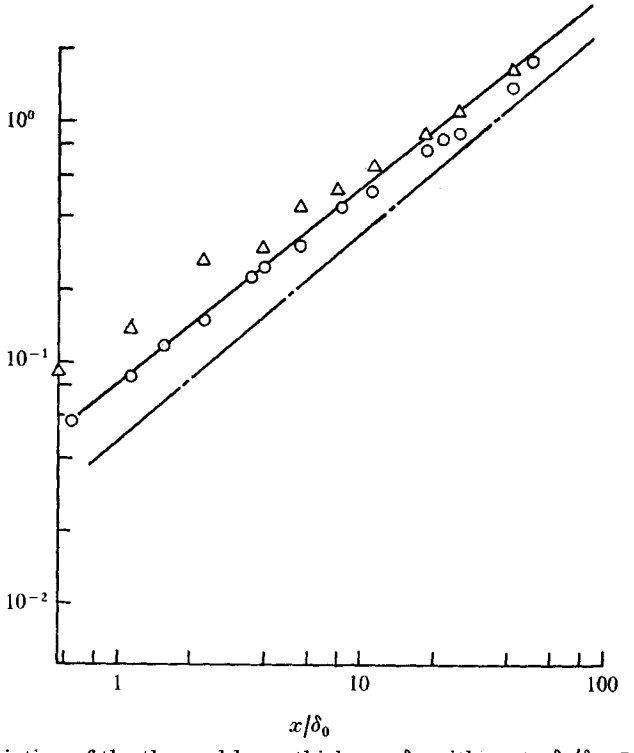

FIGURE 5. Variation of the thermal-layer thickness δ_T with x. △, δ_θ/δ_0; ○, δ_T/δ_0; ——, Townsend (1965), $l_0[\ln(l_0/z_0) - 2{\cdot}27] = 0{\cdot}34$;—·—, Bradshaw & Ferriss (1968).

The experimental variation of δ_T with x, given in figure 5, is in close agreement with the self-preserving results obtained by Townsend by integrating (6*a*) with $\kappa = 0{\cdot}41$. An alternative method for predicting the growth of the thermal layer can be obtained from the calculation method of Bradshaw & Ferriss (1968). These authors converted the exact equation for the rate of change of the mean-square temperature fluctuation along a mean streamline into an equation for $\overline{v\theta}$ which together with (5) forms a hyperbolic system of equations which is solved by the method of characteristics. The solutions are then added to the independently obtained solutions for the velocity field. If advection and diffusion of $\overline{\theta^2}$ (an equation for $\overline{\theta^2}$ is given in §5) are neglected, the equation for the outgoing characteristic from $x = 0$, which is loosely identified here with the equation for δ_T, can be written as

$$d(\delta_T)/dx = (a_{1\theta}^2 \tau)^{\frac{1}{2}}/U, \tag{9}$$

where $a_{1\theta}$, a structure function for the thermal layer, is defined by

$$a_{1\theta} = \overline{v\theta}/(\overline{\theta^2})^{\frac{1}{2}} \tau^{\frac{1}{2}}. \tag{10}$$

With U assumed to be given by (3), (9) can be integrated to yield

$$\delta_T[\ln(\delta_T/z_0) - 1] = \kappa a_{1\theta} x. \tag{11}$$

For $a_{1\theta} \simeq 0{\cdot}62$ (figure 14), the magnitude of δ_T from (11) is slightly less than that obtained from (6), but the growth rate is essentially similar to that obtained from Townsend's formulation and to the experimental growth rate $\delta_T \propto x^{0{\cdot}8}$. A similar growth rate was obtained by Antonia & Luxton (1971) for the internal layer that develops downstream of a smooth-to-rough step change in surface roughness. Also included in figure 5 is the position δ_θ of the outer edge of the $(\overline{\theta^2})^{\frac{1}{2}}$ profile, with δ_θ arbitrarily taken at the distance from the wall at which $(\overline{\theta^2})^{\frac{1}{2}} = 0{\cdot}01(T_w - T_1)$.

5. Fluctuating temperature and velocity fields

Distributions of the r.m.s. temperature fluctuations across the thermal layer are shown in figure 6 in the form $(\overline{\theta^2})^{\frac{1}{2}}/\theta_\tau$ *vs.* y/δ_T. In this form, the distributions are, somewhat surprisingly, nearly similar at all stations, with a peak value about 2·2 occurring outside the viscous sublayer, and extend slightly beyond the arbitrarily defined edge δ_T of the mean temperature profiles. Even at $x/\delta_0 = 42{\cdot}9$, there is no indication in the inner part of the layer of a region where $(\overline{\theta^2})^{\frac{1}{2}}$ changes only slowly with y, as is usually observed in the profiles of $(\overline{u^2})^{\frac{1}{2}}$ and $(\overline{v^2})^{\frac{1}{2}}$ and also in that of $(\overline{\theta^2})^{\frac{1}{2}}$ for a fully developed thermal layer (Fulachier 1972).

The normalized longitudinal heat flux $\overline{u\theta}/Q_w$ is plotted in figure 7 as a function of y/δ. Near the wall, the values of $\overline{u\theta}$ exceed Q_w by a factor of two or more. In the outer region of the thermal layer, $\overline{u\theta}$ appears to adjust fairly slowly to the new boundary condition. At the last measurement station, $x/\delta_0 \simeq 42{\cdot}9$, δ_T is only 66 % of δ and the distribution of $\overline{u\theta}/Q_w$ has not quite reached the distribution measured by Fulachier in a fully developed thermal layer. The results for the

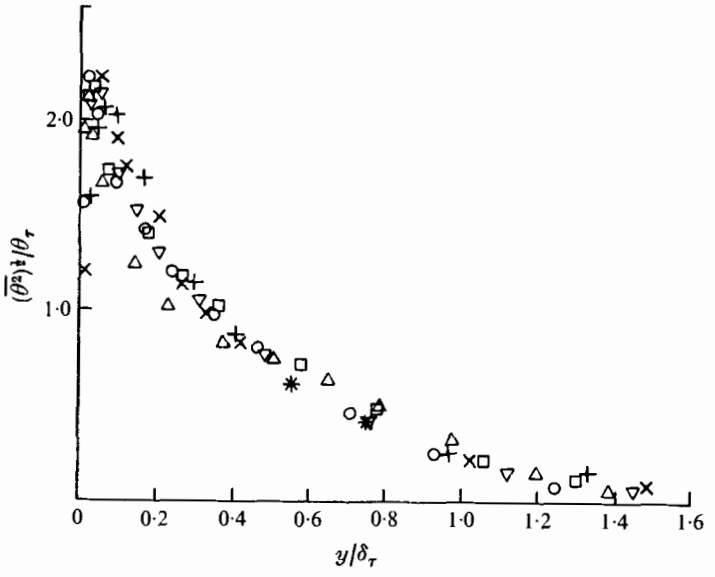

FIGURE 6. Distribution of r.m.s. temperature fluctuation across the thermal layer. +, $x/\delta_0 = 2{\cdot}3$; ×, $x/\delta_0 = 5{\cdot}7$; ▽, $x/\delta_0 = 11{\cdot}4$; ○, $x/\delta_0 = 18{\cdot}9$; □, $x/\delta_0 = 25{\cdot}7$; △, $x/\delta_0 = 42{\cdot}9$.

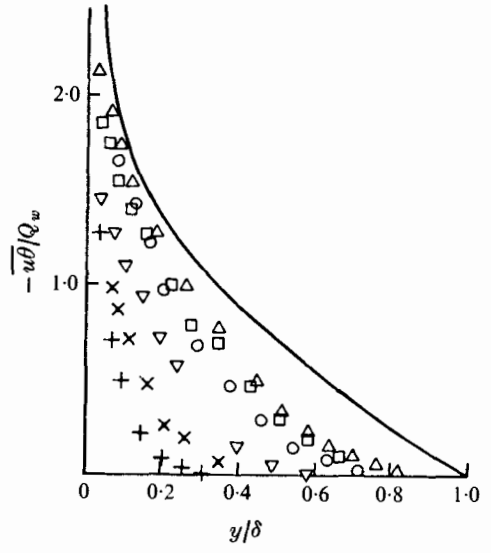

FIGURE 7. Distribution of the longitudinal heat flux as a function of y/δ. +, $x/\delta_0 = 2{\cdot}3$; ×, $x/\delta_0 = 5{\cdot}7$; ▽, $x/\delta_0 = 11{\cdot}4$; ○, $x/\delta_0 = 18{\cdot}9$; □, $x/\delta_0 = 25{\cdot}7$; △, $x/\delta_0 = 42{\cdot}9$; ——, Fulachier (1972), fully developed non-isothermal boundary layer.

transverse heat flux $\overline{v\theta}$ (figure 8) follow a trend much the same as that exhibited by $\overline{u\theta}$ in figure 7. It is worth noting that there is no region where $\overline{v\theta}$ is approximately constant (the contribution from the term $k\,\partial T/\partial y$, left out in (5), to the total heat flux is significant only in the viscous sublayer). This is in direct contrast to the measurements of $\overline{uv}$, which vary only slightly in the region $y/\delta < 0{\cdot}10$. The fairly large gradients in $\overline{v\theta}$ at small x/δ_0 reflect the importance of the term

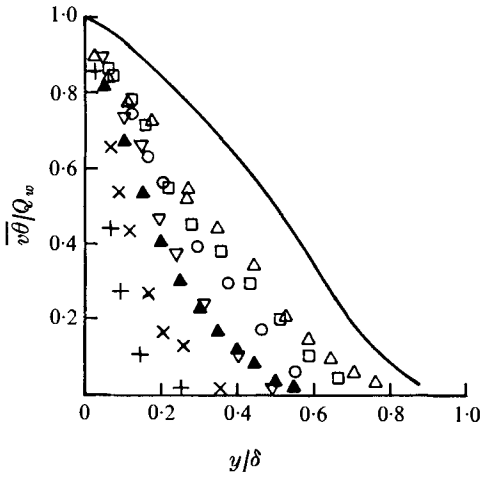

FIGURE 8. Transverse heat flux distributions as a function of y/δ. ▲, $x/\delta_0 = 10{\cdot}3$ (Fulachier, step change in temperature); other symbols as in figure 7.

$U\,\partial T/\partial x$ in (5) in the region near the step. The closed symbols in figure 11 are the values measured by Fulachier at $x/\delta_0 \simeq 10{\cdot}3$ downstream of a step in wall temperature. They are in reasonable agreement with the present results at $x/\delta_0 \simeq 11{\cdot}4$.

When δ_T is used instead of δ as the normalizing length scale, the similarity of distributions of $\overline{v\theta}$ (figure 9) appears reasonable within the scatter in the data. The self-preserving solution for $\overline{v\theta}$ [equation (8)] is not in good agreement with the data, as it generally underestimates the experimental values for $\eta < 0{\cdot}8$ and overestimates them near the edge of the thermal layer. This disagreement is likely to be a result of the failure of the experimental situation to satisfy the assumption in Townsend's analysis. The ratio $-\overline{u\theta}/\overline{v\theta}$, plotted in figure 10, demonstrates the near similarity of $\overline{u\theta}$ at all stations except perhaps those at large values of x, where $\overline{u\theta}$ increases near the wall.

The equation for $\overline{\theta^2}$ along a mean streamline in a turbulent shear flow can be written (e.g. Corrsin 1953) as

$$U_i\frac{\partial\overline{\theta^2}}{\partial x_i}+2\overline{\theta u_i}\frac{\partial\overline{T}}{2x_i}+\frac{\partial}{\partial x_i}\overline{(u_i\theta^2)}-\alpha\frac{\partial^2\overline{\theta^2}}{\partial x_i^2}+2\alpha\overline{\left(\frac{\partial\theta}{\partial x_i}\right)\left(\frac{\partial\theta}{\partial x_i}\right)}=0 \tag{12}$$

or

$$\underbrace{U\frac{\overline{\partial\theta^2}}{\partial x}+V\frac{\overline{\partial\theta^2}}{\partial y}}_{\text{I advection}}+\underbrace{2\overline{\theta u}\frac{\partial T}{\partial x}+2\overline{\theta v}\frac{\partial T}{\partial y}}_{\text{II production}}+\underbrace{\frac{\partial}{\partial x}\overline{(u\theta^2)}+\frac{\partial}{\partial y}\overline{(v\theta^2)}}_{\text{III diffusion}}-\underbrace{\alpha\frac{\partial^2\overline{\theta^2}}{\partial x^2}-\alpha\frac{\partial^2\overline{\theta^2}}{\partial y^2}}_{\text{IV molecular dissipation}}$$

$$+2\alpha\underbrace{\left[\overline{\left(\frac{\partial\theta}{\partial x}\right)^2}+\overline{\left(\frac{\partial\theta}{\partial y}\right)^2}+\overline{\left(\frac{\partial\theta}{\partial z}\right)^2}\right]}_{\text{V dissipation or destruction}}=0. \tag{13}$$

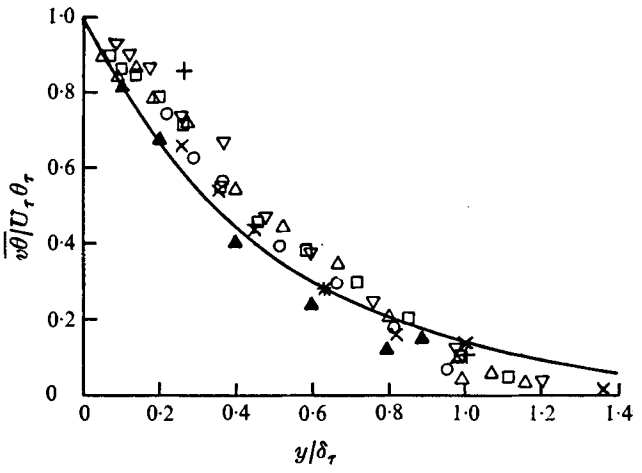

FIGURE 9. Transverse heat flux distribution in the thermal layer. Symbols as for figure 8; ——, Townsend (1965), $\phi_1 = e^{-2\eta}$.

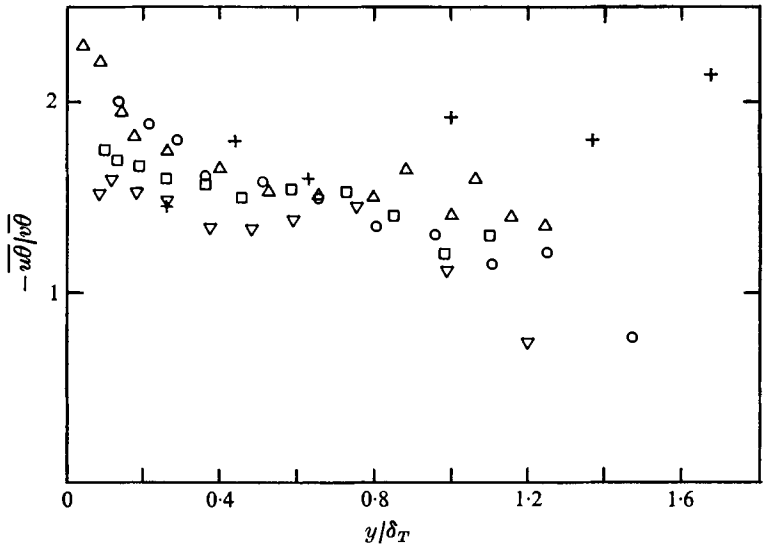

FIGURE 10. Distributions of ratio $\overline{u\theta}/\overline{v\theta}$ in the thermal layer. Symbols as for figure 7.

The first terms in expressions II–IV are found to be small at all values of x and can be ignored in the present situation. The distributions of other terms in (13), made dimensionless by multiplication by $\delta_T/U_\tau\theta_\tau^2$, are shown in figures 11 (*a*), (*b*) and (*c*) for $x/\delta_0 = 2{\cdot}3$, 11·4 and 42·9 respectively. At $x/\delta_0 = 2{\cdot}3$, both the advection (I) and the diffusion (III) are of the same order of magnitude as the dissipation or destruction term (V) but the imbalance, or the amount by which (13) fails to close, is not small in the outer region of the thermal layer, being approximately equal to the dissipation or diffusion terms.† As x increases, the diffusion and

† As a result of this relatively large imbalance (due mainly to the difficulty in making reliable measurements in the thermal layer at this small value of x), the implications of figure 11 (*a*), such as a large gain by diffusion in the region very close to the wall, cannot be trusted.

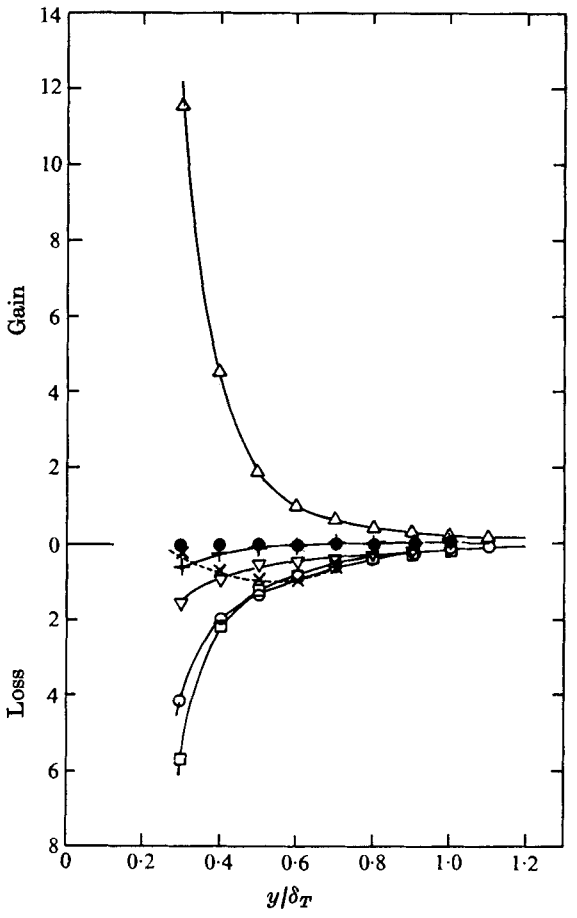

FIGURE 11(*a*). For caption see p. 167.

advection terms decrease in magnitude, at least in the inner region of the flow, and the magnitude of the imbalance in figures 11(*b*) and (*c*) is satisfactorily small. At $x/\delta_0 = 42{\cdot}9$, the advection is negligible while the dissipation is only marginally smaller than the production in the inner layer, indicating that production and destruction of temperature fluctuations are very nearly in balance in this region. The requirement that

$$\int_0^\infty \frac{\partial(\overline{v\theta^2})}{\partial y}\,dy$$

should be zero seems to be reasonably satisfied at $x/\delta_0 = 42{\cdot}9$. The general difficulty of accurately estimating the diffusion term (this is especially true at $x/\delta_0 = 2{\cdot}3$, where δ_T is only 0·69 cm) is considered to be a major reason for the non-zero imbalance in figures 11(*a*)–(*c*).

The dissipation $\chi = 2\alpha\overline{(\partial\theta/\partial x_i)(\partial\theta/\partial x_i)}$ was here assumed to be equal to $3\alpha[\overline{(\partial\theta/\partial x)^2} + \overline{(\partial\theta/\partial y)^2}]$. The components $\partial\theta/\partial x$ and $\partial\theta/\partial y$ were obtained with two parallel wires (90% Pt/10% Rh, 0·6 μm in diameter, 0·6 mm long†) placed

† The temperature coefficient of resistivity for these wires was 0·0015 °C^{-1}.

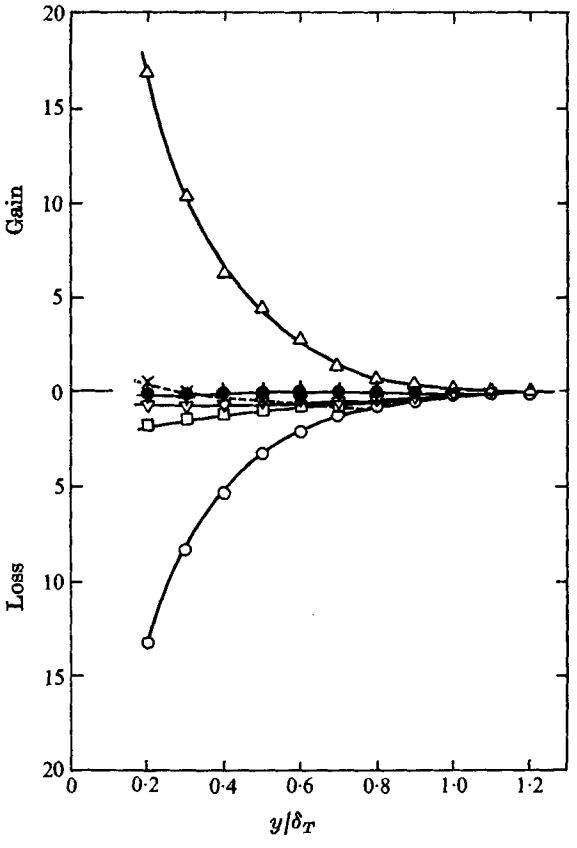

FIGURE 11 (*b*). For caption see p. 167.

perpendicular to the flow and parallel to the wall. The streamwise derivative $\partial\theta/\partial x$ was obtained from the time derivative of one of the temperature signals, with the use of Taylor's hypothesis. The fluctuation $\partial\theta/\partial y$ was approximated by the ratio $\Delta\theta/\Delta y$, where $\Delta\theta$ is the difference between the two signals and Δy ($\simeq 0{\cdot}7$ mm) is the separation between the wires.† The fluctuation $\partial\theta/\partial z$ was measured (with the wires perpendicular to the wall) only at $x/\delta_0 = 42{\cdot}9$ and the results at this station indicated that $\overline{(\partial\theta/\partial z)^2} \simeq \frac{1}{2}[\overline{(\partial\theta/\partial x)^2} + \overline{(\partial\theta/\partial y)^2}]$. At all stations, $\overline{(\partial\theta/\partial y)^2}$ was found to be slightly larger than $\overline{(\partial\theta/\partial x)^2}$, by about 5–25%. The lower values of $\overline{(\partial\theta/\partial x)^2}$ compared with $\overline{(\partial\theta/\partial y)^2}$ or $\overline{(\partial\theta/\partial z)^2}$ might explain the low values of the dissipation (figure 11*a*) derived from Fulachier's λ_θ values with the use of the isotropic relation $\chi = 6\alpha\overline{\theta^2}/\lambda_\theta^2$, where λ_θ is the length scale $(\overline{\theta^2}/\overline{(\partial\theta/\partial x)^2})^{\frac{1}{2}}$, analogous to the Taylor microscale.

† In the χ results in figure 11, no attempt was made to account for the attenuation of the high frequency end of the dissipation spectrum as a result of the finite length of the wires (or the finite separation between the wires). At $y/\delta_T = 0{\cdot}2$, the wire length l_w ($\simeq 0{\cdot}6$ mm) is about $4l_\kappa$, where l_κ is the Kolmogorov microscale. For this value of l_w, Wyngaard's (1971) calculations, based on a particular shape of the temperature spectrum for isotropic turbulence, estimate that the measured values of χ could be lower than the true values by about 15%.

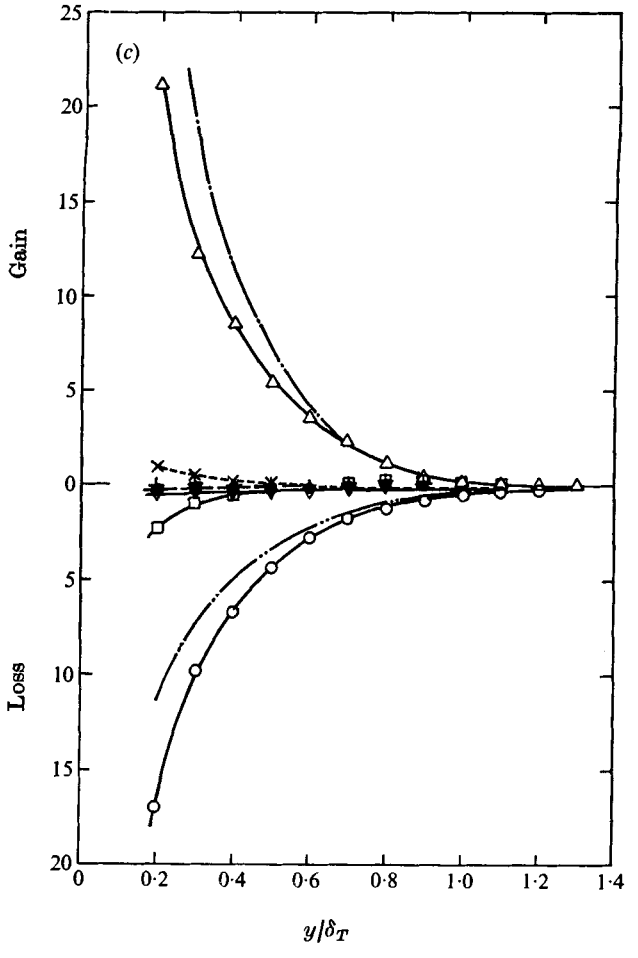

FIGURE 11. Budget of $\overline{\theta^2}$ across the thermal layer at three streamwise stations. △, production [term II in (13)]; □, diffusion (III); ▽, advection (I); ○, destruction or dissipation (V); ●, molecular dissipation (IV); +, molecular transport; ×, imbalance. (All terms are normalized by $\delta_T/\theta_\tau^2 U_\tau$.) Fulachier's (1972) results: —·—, production; —· · —, dissipation. (*a*) $x/\delta_0 = 2{\cdot}3$; (*b*) $x/\delta_0 = 11{\cdot}4$; (*c*) $x/\delta_0 = 42{\cdot}9$.

A dissipation length scale L_χ for the temperature fluctuations can be defined as (Bradshaw & Ferriss 1968) $L_\chi = \overline{(v\theta)^2}/\chi\tau^{\frac{1}{2}}$, which becomes identical to the mixing length l_θ [equation (7)] when the production and dissipation of $\overline{\theta^2}$ are equal. The variation of L_χ/δ_T over the layer, given in figure 12, shows that L_χ/δ_T is fairly high at small values of x but rapidly decreases as x increases. For $x/\delta_0 > 11{\cdot}4$, the values of L_χ near the wall lie fairly close to the line $\kappa_\theta y$, as the inner region of the thermal layer is nearly in equilibrium. The trend in the mixing-length results in figure 13 indicates a decrease in l_θ/δ_T in the outer part of the layer as x increases. Near the wall, l_θ does not depart significantly from the line $\kappa_\theta y$ except perhaps at the first station, whilst near the edge of the thermal layer, it shows a sharp rise, similar to the distribution of l but in contrast to the decreasing trend in L_χ. It

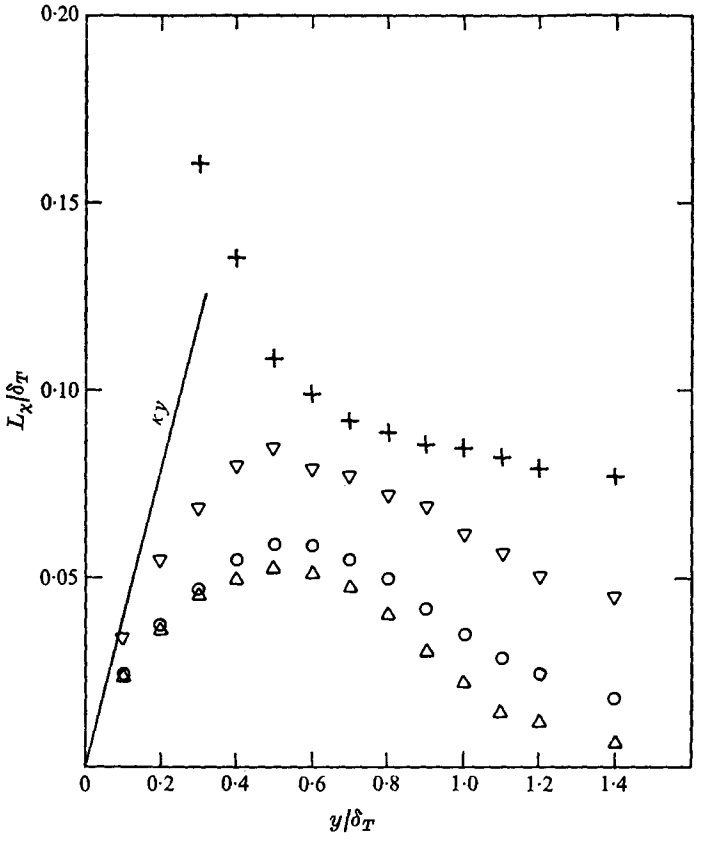

FIGURE 12. Dissipation length scale L_χ/δ_T for the temperature fluctuations in the thermal layer. +, $x/\delta_0 = 2{\cdot}3$; ∇, $x/\delta_0 = 11{\cdot}4$; ○, $x/\delta_0 = 18{\cdot}9$; △, $x/\delta_0 = 42{\cdot}9$.

seems likely that the variation of the length scale L_χ with x must be included in any calculation method for the thermal layer, particularly if the heat-transfer characteristics immediately downstream of the step are to be correctly evaluated. In the method of Bradshaw & Ferriss (1968), L_χ was assumed to be equal to L_ϵ/Pr_t in the fully turbulent part of the flow, where $L_\epsilon = \tau^{\frac{3}{2}}/\epsilon$ is the turbulent energy dissipation length scale. This assumption is, as pointed out by these authors, valid only when neither the thermal layer nor the velocity boundary layer is changing rapidly. It is worth noting that one of the other assumptions in the method of Bradshaw & Ferriss, namely the assumed constancy of the parameter $a_{1\theta}$ [equation (10)], seems to be supported by the present data (figure 14) for $x/\delta_0 \geqslant 5{\cdot}7$. Near the step, $a_{1\theta}$ is approximately constant over most of the thermal layer but its magnitude is slightly larger than at larger x/δ_0, where it is approximately 0·62, which is slightly less than that of Fulachier (0·75) but larger than that used by Bradshaw & Ferriss ($\simeq 0{\cdot}4$).

The turbulent Prandtl number Pr_t, defined as the ratio $\overline{uv}(\partial T/\partial y)/\overline{v\theta}(\partial U/\partial y)$ of momentum diffusivity to thermal diffusivity, has been evaluated from the present data at several stations and is shown in figure 15. Although the experimental uncertainty in the derivation of Pr_t is unavoidably large and partly

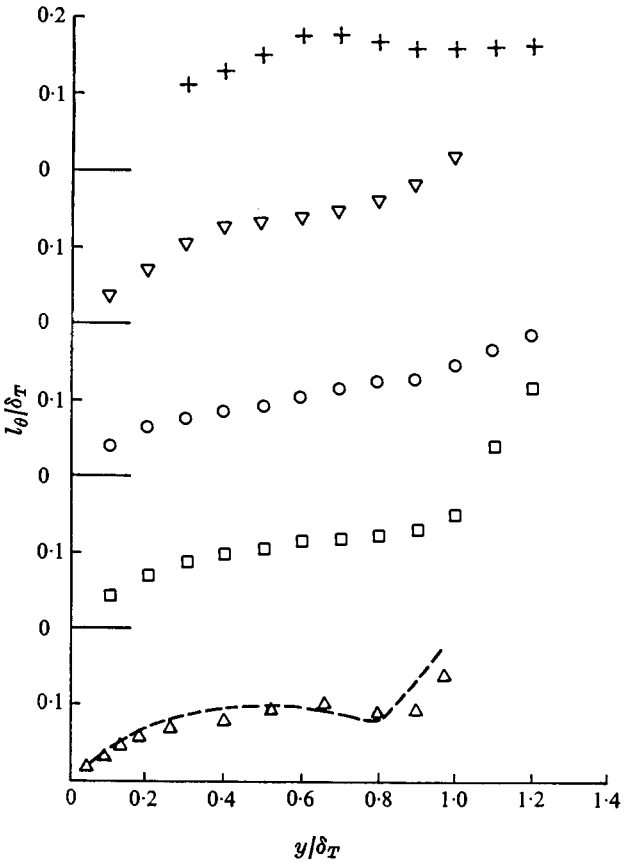

FIGURE 13. Thermal mixing length l_θ across the thermal layer. □, $x/\delta_0 = 25{\cdot}7$. Other symbols are as for figure 12. — —, Fulachier (1972), fully developed boundary layer.

responsible for the large scatter in the Pr_t data presented in the literature (see Blom 1970), the main features of the distributions in figure 15 are consistent with the data presented in the previous sections for the mean and fluctuating temperature fields. Values of Pr_t well in excess of one are obtained only at $x/\delta_0 = 2{\cdot}3$, over the central and outer regions of the layer, but, when allowance is made (cf. §6) for the temperature 'intermittency' of the thermal layer, the resulting distribution is not much different from that at stations further downstream. In the region near the wall, there is a general tendency (except for the results at $x/\delta_0 = 25{\cdot}7$) for Pr_t to be slightly higher than one. In the inner region of the layer, $\partial T/\partial y \simeq \theta_\tau/\kappa_\theta y$ and $\partial U/\partial y \simeq U_\tau/\kappa y$, and as $\kappa_\theta \simeq \kappa$ in the present case, values of Pr_t greater than unity are consistent with the observation that $\overline{v\theta}/U_\tau\theta_\tau < \overline{uv}/U_\tau^2$ over most of the inner region. This inequality is also evident in the measurements of Verollet & Fulachier (1969), even when the velocity and thermal layers are identical, but there is a compensating effect, in their case, due to $\kappa_\theta > \kappa$.

The trend of the present Pr_t variation in the outer layer is in better agreement

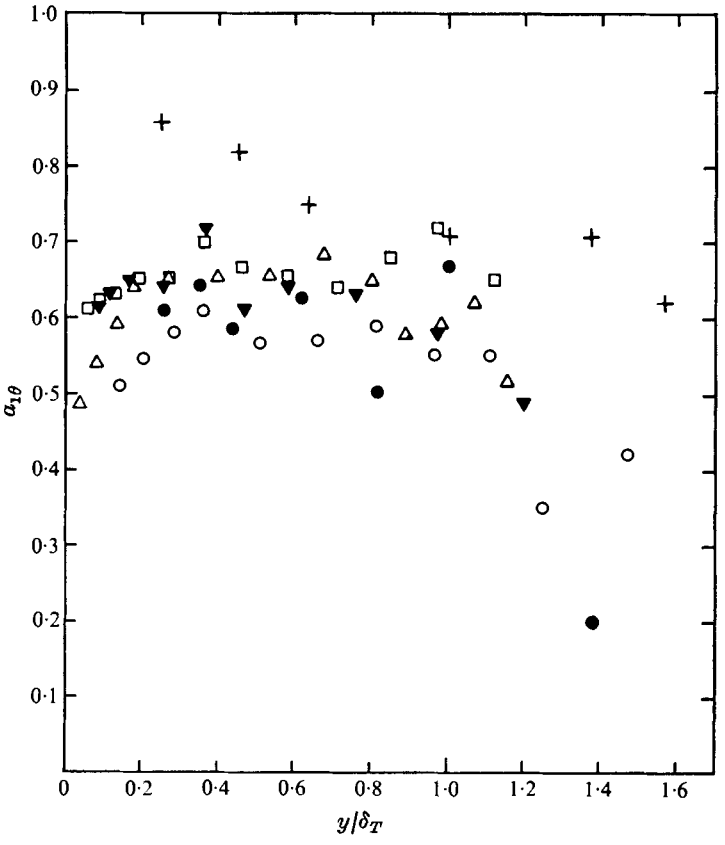

FIGURE 14. Variation of parameter $a_{1\theta}$ across the thermal layer. +, $x/\delta_0 = 2{\cdot}3$; ●, $x/\delta_0 = 5{\cdot}7$; ▼, $x/\delta_0 = 11{\cdot}4$; ○, $x/\delta_0 = 18{\cdot}9$; □, $x/\delta_0 = 25{\cdot}7$; △, $x/\delta_0 = 42{\cdot}9$.

with that of Fulachier (1972) than with that of Blom (1970), which was obtained from measured values of $\overline{uv}$ and $\overline{v\theta}$. When Blom used values of $\overline{uv}$ and $\overline{v\theta}$ calculated from the mean velocity and temperature profiles, Pr_t showed an increase in the outer layer.

6. Statistics of thermal-layer interface

To obtain a measure of some of the statistical quantities associated with the thermal-layer interface, it was necessary to form the intermittency function $I(t)$ as an indicator of the passage of the interface. The method for generating $I(t)$ is similar to that used in Antonia *et al.* (1975). Whenever the instantaneous temperature exceeded the ambient air temperature by an amount T_H, I was set equal to one. The use of the threshold T_H was necessary to allow for the noise level of the anemometer signal. The use of a hold time (LaRue 1974; Ali & Kovasznay 1974) during which the temperature is compared with T_H to avoid spurious indications by $I(t)$ was not required here. The variation of the mean value $\bar{I}$ and crossing frequency f_γ of $I(t)$ with T_H at several positions in the thermal layer was found

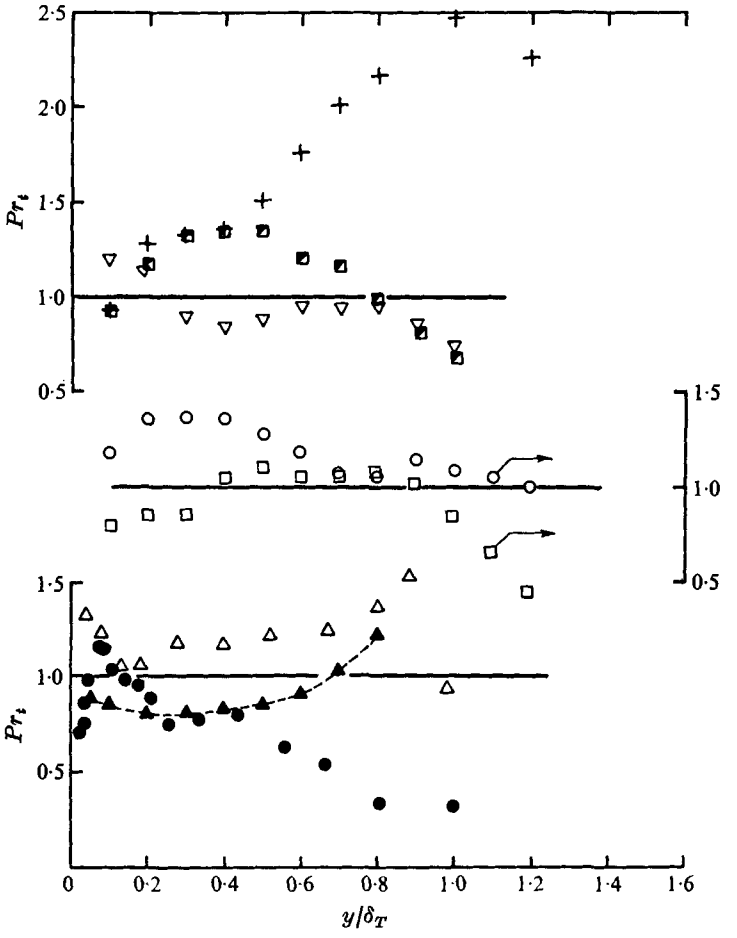

FIGURE 15. Turbulent Prandtl number across the thermal layer. ◪, present conditional measurement at $x/\delta_0 = 2{\cdot}3$; ▲, Fulachier (1972), fully developed boundary layer; ●, Blom (1970). Other symbols are as for figure 12.

to be qualitatively similar to that reported in Antonia *et al.* (1975). A suitable choice of T_H inferred from this variation was found to be in good agreement with the setting of T_H obtained by visual comparison of $I(t)$ and temperature traces on a storage oscilloscope. It should be emphasized here that the setting $I = 0$ does not necessarily indicate that the flow field is irrotational. At small values of x, $I = 0$ corresponds almost invariably to a fully turbulent velocity field, whilst for larger values of x, the velocity field outside the thermal interface has the intermittent features associated with the velocity-layer interface. When the thermal layer eventually reaches the edge of the boundary layer, a condition which is not attained in the present experiment, $I = 0$ can be interpreted to indicate irrotational flow, provided that the thermal interface is assumed to coincide exactly with the turbulent/non-turbulent interface.

The intermittency factor $\gamma = \bar{I}$, here understood to mean the fraction of time for which the flow is heated, is plotted in figure 16 as a function of y/δ_T, for

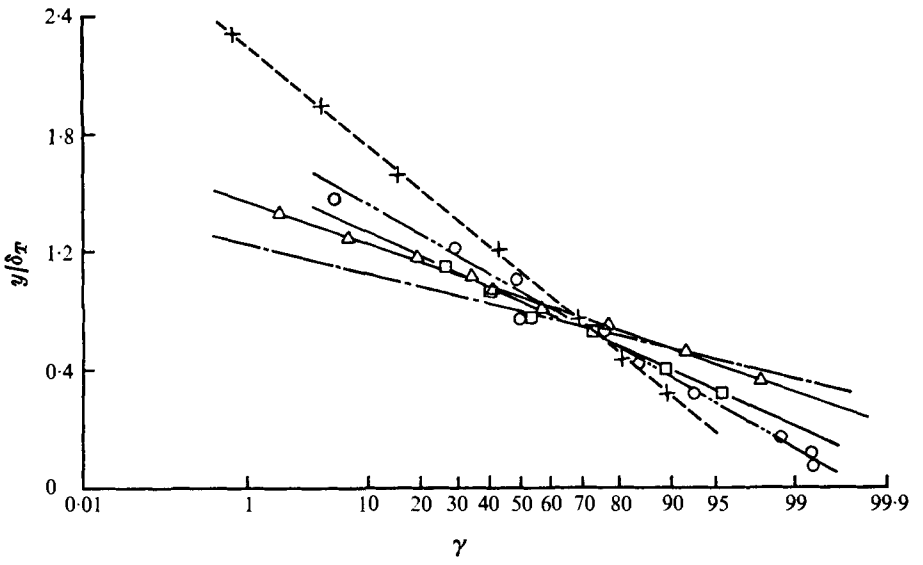

FIGURE 16. Intermittency factor γ across the thermal layer at different stations on linear probability paper. +, $x/\delta_0 = 2{\cdot}3$; ○, $x/\delta_0 = 19{\cdot}8$; □, $x/\delta_0 = 25{\cdot}7$; △, $x/\delta_0 = 42{\cdot}9$; —·—, Dumas *et al.* (1972), fully developed boundary layer.

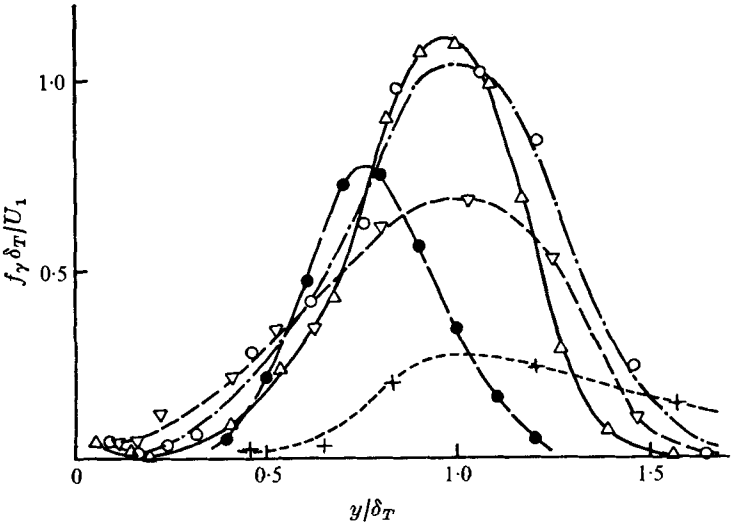

FIGURE 17. Interface frequency distributions $f_\gamma \delta_T/U_1$ in the thermal layer at different stations. +, $x/\delta_0 = 2{\cdot}3$; ▽, $x/\delta_0 = 11{\cdot}4$; ○, $x/\delta_0 = 18{\cdot}9$; △, $x/\delta_0 = 42{\cdot}9$; ●, ——, Kovasznay *et al.* (1970), fully developed isothermal boundary layer.

different values of x. The results on the linear probability plot follow a linear variation fairly closely, even at the smallest values of x. The mean position of the interface thus appears to be normally distributed with $\gamma = 0{\cdot}5$ corresponding to $y/\delta_T = 1$. Also, $y \simeq \delta_T$ corresponds approximately to the position of a maximum in the interface frequency distributions of figure 17 for all values of x.

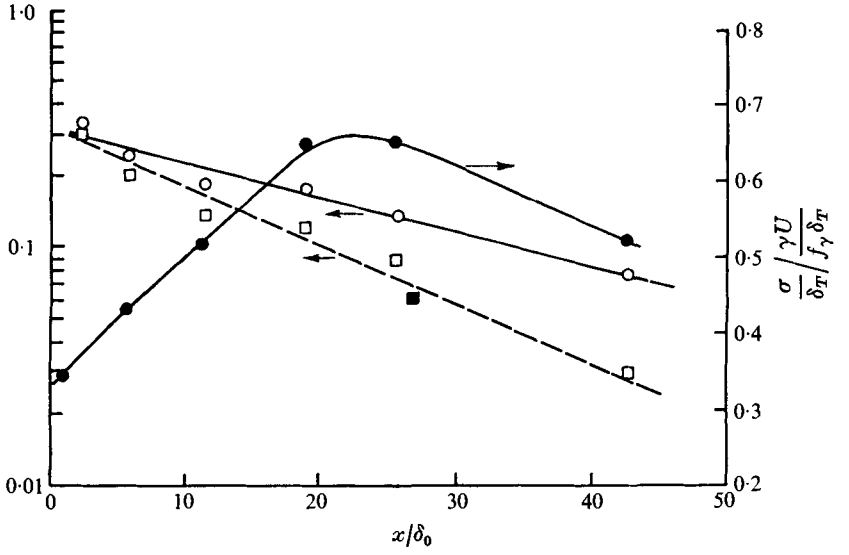

FIGURE 18. Variation of standard deviation and roughness of thermal interface with x. ○, $\sigma/\delta_T - 0{\cdot}15$; □, $\sigma/\delta_T - 0{\cdot}19$; ■, Johnson (1959), developing non-isothermal boundary layer, $\sigma/\bar{y} - 0{\cdot}19$; ●, $(\sigma/\delta_T)/(\gamma U/f_\gamma \delta_T)$.

These results appear to provide some *a posteriori* justification for our choice of δ_T as representative of the edge of the thermal layer. The standard deviation σ of the interface decreases markedly with increasing x (figure 16). At $x/\delta_0 = 2{\cdot}3$, $\sigma/\delta_T \simeq 0{\cdot}50$ whilst at the last measurement station $\sigma/\delta_T (\simeq 0{\cdot}22)$ is still significantly higher than the value of $\sigma/\delta \simeq 0{\cdot}15$ commonly reported in the literature (e.g. Klebanoff (1955) or Kovasznay, Kibens & Blackwelder (1970) for a fully developed isothermal layer and Dumas, Fulachier & Arzoumanian (1972) for a fully developed non-isothermal layer).† Johnson's (1959) distribution of γ deviates significantly from the Gaussian at small and large values of y/δ_T but is also characterized by a high value of σ ($\simeq 0{\cdot}25\delta_T$).

The maximum value of $f_\gamma \delta_T/U_1$ (figure 17) increases fairly rapidly with x for small values of x. At $x/\delta_0 = 42{\cdot}9$, $(f_\gamma \delta_T/U_1)_{\max} \simeq 1{\cdot}1$, which is identical with the value of $(f_\gamma \delta/U_1)_{\max}$ obtained by Hedley & Keffer (1974), but significantly larger than the value of 0·76 reported in Kovasznay *et al.* (1970) and Charnay (1974). It must be noted however that Hedley & Keffer's value is probably less reliable than that of Kovasznay *et al.* because of the anomalously low 'wake' component of the mean velocity profile reported in Hedley & Keffer. Another feature of figure 17 is the lack of symmetry of the distributions, which, after showing a positive skewness at the first station, remain negatively skewed downstream with the magnitude of the skewness decreasing with increasing x. The difference

† Note here that this decrease in σ/δ_T with increasing x appears to be compatible with the increase in σ/δ in the case of a slightly heated turbulent boundary layer subjected to increasing levels of free-stream turbulence (Charnay *et al.* 1972). The analogy must however be considered with caution since, in the present flow, the thermal layer develops under an external stream with, at least initially, relatively high levels of turbulence and shear.

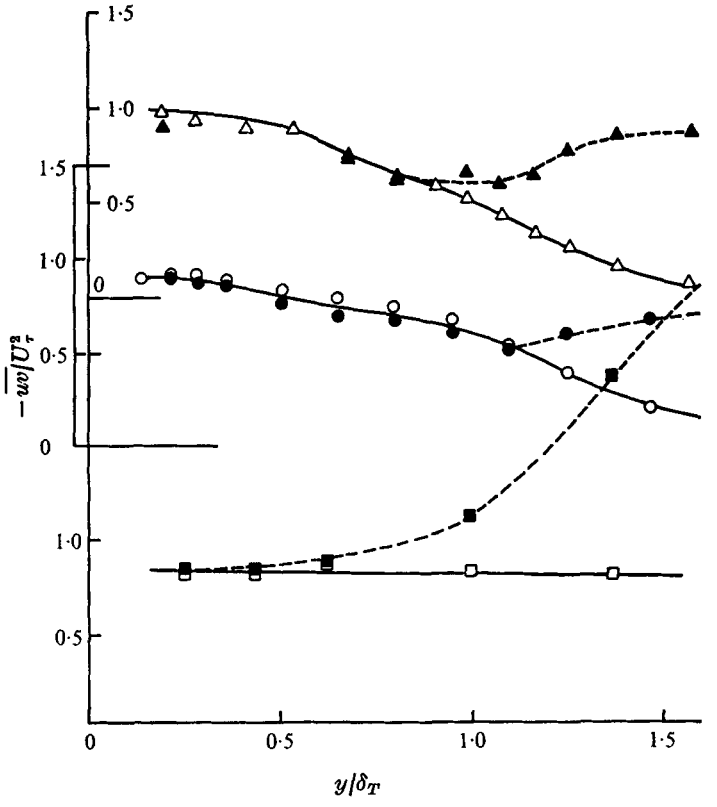

FIGURE 19. Conventional and conditional averages of Reynolds shear stress $\overline{uv}/U_\tau^2$ in the thermal layer. Conventional: □, $x/\delta_0 = 2{\cdot}3$; ○, $x/\delta_0 = 18{\cdot}9$; △, $x/\delta_0 = 42{\cdot}9$. Filled symbols refer to conditional averages $-(\overline{uv})_h/U_\tau^2$ in the heated flow only.

between σ/δ_T and the 'fully developed' value of 0·15 is plotted *vs.* x in figure 18 in an attempt to obtain a rough indication of the rate of approach of the present flow to the fully developed condition. The difference (figure 18) appears to decay exponentially,† i.e. $(\sigma/\delta_T - 0{\cdot}15) \sim e^{-x/X}$, where $X \simeq 350$ cm ($X/\delta_0 \simeq 79$). As δ_T appears to be closely related to the mean position, $\bar{y}$ say, of the interface and $\bar{y}/\delta \simeq 0{\cdot}8$ in a fully developed layer, the difference $\sigma/\delta_T - 0{\cdot}19$ yields a value of $X/\delta_0 = 20$. We have estimated that the edge δ_T of the thermal layer intersects δ at $x/\delta_0 = 90$, assuming that extrapolation of δ_T (figure 5) to larger values of x is permissible. This result, together with the above values of X/δ_0, suggests that a distance of order $100\delta_0$ ($\simeq 1000\theta_0$) might be required to achieve fully developed conditions in the thermal layer.

Some indication of the 'roughness' of the interface is given in figure 18 by the ratio $(\sigma/\delta_T)/(\gamma U/f_\gamma \delta_T)$, the numerator and denominator roughly representing a typical amplitude and mean width respectively of the interface.‡ This ratio, shown in figure 18 for $\gamma = 0{\cdot}5$, is low at small x as the relatively large values of σ

† There is no physical justification for the exponential decay.

‡ An analogous parameter was used by Wygnanski & Fiedler (1970) to characterize the interfaces of a mixing layer.

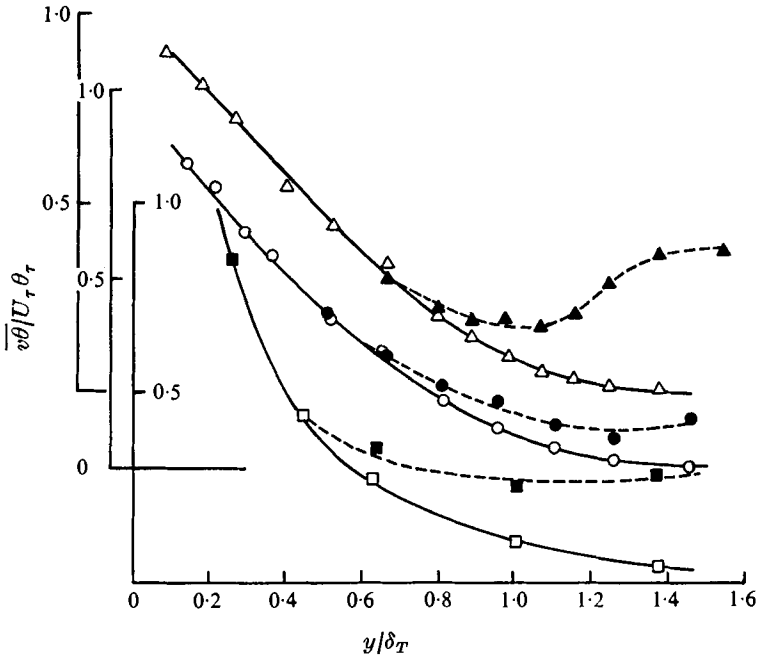

FIGURE 20. Conventional and conditional averages of the Reynolds heat flux $\overline{v\theta}/\theta_\tau U_\tau$. Symbols as for figure 19.

are offset by the very low values of f_γ. The 'roughness' has a maximum near $x/\delta_0 \simeq 22$ and then decreases fairly rapidly with increasing x. From the measurements of Kovasznay *et al.* (1970), the value of this ratio for a fully developed boundary layer is 0·23 (for $\gamma = 0{\cdot}5$).

Conditional and conventional values of the Reynolds shear stress $\overline{uv}$ and heat fluxes $\overline{v\theta}$ and $\overline{u\theta}$ are shown in figures 19–21. The subscript h is used to denote zone averages in the 'hot' part of the flow. The interesting feature of figure 20 is the relatively large value of $(-\overline{uv})_h$ near the step. The difference between $(-\overline{uv})_h$ and $-\overline{uv}$ at $x/\delta_0 = 2{\cdot}3$ exceeds the local shear stress by a factor greater than τ_w at larger values of y/δ_T. This difference seems to be associated with fairly large values of $\overline{u}_h$ (negative) and $\overline{v}_h$ (positive) and is consistent with the idea of 'bursts' of low momentum fluid which are tagged by the passive scalar contaminant. The relatively large values of $(\overline{uv})_h$ at $x/\delta_0 = 2{\cdot}3$ are offset by even larger values of $(\overline{v\theta})_h$, so that the Prandtl number

$$(\overline{uv})_h(\partial\overline{T}_h/\partial y)/(\overline{v\theta})_h(\partial\overline{U}_h/\partial y)$$

in the heated part of the fluid is significantly lower than the conventional Prandtl number (figure 15). At a given value of y/δ_T, the difference $\overline{uv} - (\overline{uv})_h$ is smaller at $x/\delta_0 = 18{\cdot}9$ than at $x/\delta_0 = 2{\cdot}3$ and increases again at $x/\delta_0 \simeq 42{\cdot}9$. This trend is also observable in $(\overline{v\theta})_h - \overline{v\theta}$ (figure 20) and, to a lesser extent, in $\overline{u\theta} - (\overline{u\theta})_h$ (figure 21). The original decrease at small values of x in the magnitude of the conditional averages of the momentum and heat fluxes relative to their

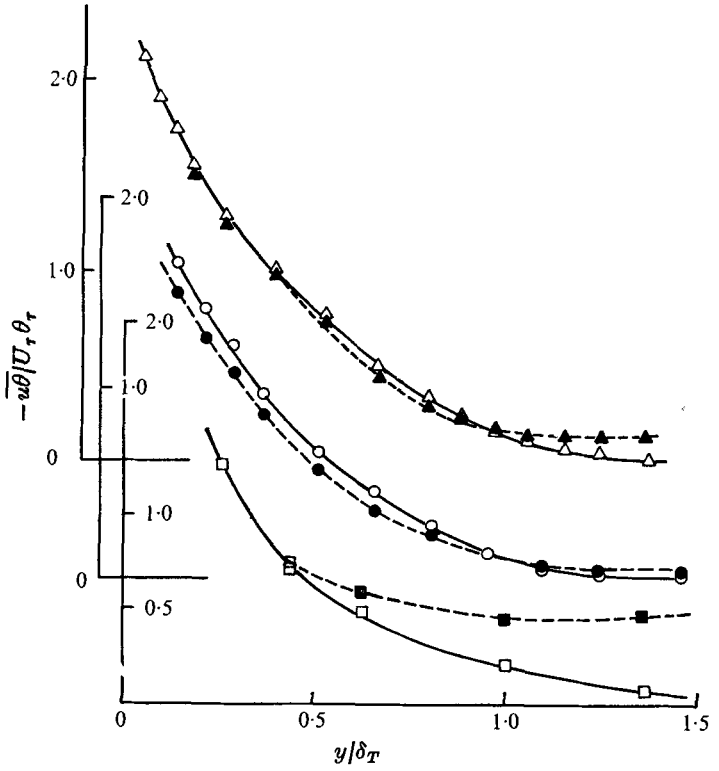

FIGURE 21. Conventional and conditional averages of the Reynolds heat flux $\overline{u\theta}/\theta_\tau U_\tau$. Symbols as for figure 19.

conventional averages is probably a result of the loss in identity of the 'bursts' (e.g. Kline *et al.* 1967) as the distance from the wall increases and also of the presence of highly turbulent fluid outside the interface. Well downstream from the step the difference between conventional and conditional averages increases again as the probability of occurrence of non-turbulent fluid outside the interface increases and as the scalar contaminant becomes an effective marker of the large-scale structure of the flow.

The work described in this paper represents part of a programme of research supported by the Australian Research Grants Committee and the Australian Institute of Nuclear Science and Engineering.

REFERENCES

ALI, S. F. & KOVASZNAY, L. S. G. 1974 Approach to self-preservation in a heated wake behind a flat plate. *A.S.M.E. Paper*, 74-WA/HT-35.

ANTONIA, R. A. 1972 Conditionally sampled measurements near the outer edge of a turbulent boundary layer. *J. Fluid Mech.* **56**, 1.

ANTONIA, R. A. & ATKINSON, J. D. 1974 Use of a pseudo-turbulent signal to calibrate an intermittency measuring circuit. *J. Fluid Mech.* **64**, 679.

ANTONIA, R. A. & LUXTON, R. E. 1971 The response of a turbulent boundary layer to a step change in surface roughness. Part 1. Smooth to rough. *J. Fluid Mech.* **48**, 721.

ANTONIA, R. A., PRABHU, A. & STEPHENSON, S. E. 1975 Conditionally sampled measurements in a heated turbulent jet. *J. Fluid Mech.* **72**, 455.

BLOM, J. 1970 Experimental determination of the turbulent Prandtl number in a developing temperature boundary layer. *4th Int. Heat Transfer Conf., Paris–Versailles*, vol. II, paper FC2.2.

BRADSHAW, P. & FERRISS, D. H. 1968 Calculation of boundary layer development using the turbulent energy equation. IV. Heat transfer with small temperature differences. *Nat. Phys. Lab. Rep.* no. 1271.

BRADSHAW, P., FERRISS, D. H. & ATWELL, N. P. 1967 Calculation of boundary-layer development using the turbulent energy equation. *J. Fluid Mech.* **28**, 593.

CHARNAY, G. 1974 Caractéristique d'une couche limite turbulente évoluant en présence d'un écoulement extérieur turbulent. Thèse Docteur ès Sciences, Université Claude Bernard, Lyon.

CORRSIN, S. 1953 Remarks on turbulent heat transfer. *Proc. 1st Iowa Symp. Thermodyn., State University of Iowa.*

DUMAS, R., FULACHIER, L. & ARZOUMANIAN, E. 1972 Facteurs d'intermittence et de dissymétrie des fluctuations de température et de vitesse dans une couche limite turbulente. *C. R. Acad. Sci. Paris*, A **274**, 267.

FULACHIER, L. 1972 Contribution à l'étude des analogies des champs dynamique et thermique dans une couche limite turbulente. Effet de l'aspiration. Thèse Docteur ès Sciences, Université de Provence.

HEDLEY, T. B. & KEFFER, J. F. 1974 Some turbulent/non-turbulent properties of the outer intermittent region of a boundary layer. *J. Fluid Mech.* **64**, 645.

JOHNSON, D. S. 1957 Velocity, temperature and heat transfer measurements in a turbulent boundary layer downstream of a stepwise discontinuity in wall temperature. *J. Appl. Mech., Trans. A.S.M.E.* **24**, 2.

JOHNSON, D. S. 1959 Velocity and temperature fluctuation measurements in a turbulent boundary layer downstream of a stepwise discontinuity in wall temperature. *J. Appl. Mech., Trans. A.S.M.E.* **26**, 325.

KAYS, W. M. 1966 *Convective Heat and Mass Transfer*. McGraw-Hill.

KLEBANOFF, P. S. 1955 Characteristics of turbulence in a boundary layer with zero pressure gradient. *N.A.C.A. Rep.* no. 1247.

KLINE, S. J., REYNOLDS, W. C., SCHRAUB, F. A. & RUNSTADLER, P. W. 1967 The structure of turbulent boundary layers. *J. Fluid Mech.* **30**, 741.

KOVASZNAY, L. S. G., KIBENS, V. & BLACKWELDER, R. F. 1970 Large-scale motion in the intermittent region of a turbulent boundary layer. *J. Fluid Mech.* **41**, 283.

LARUE, J. C. 1974 Detection of the turbulent–nonturbulent interface in slightly heated turbulent shear flows. *Phys. Fluids*, **17**, 1513.

STELLEMA, L., ANTONIA, R. A. & PRABHU, A. 1975 A constant current resistance thermometer for the measurement of mean and fluctuating temperatures in turbulent flows. *Charles Kolling Res. Lab., Dept. Mech. Engng, Univ. Sydney, Tech. Note*, D-12.

SWENSON, G. G. 1973 The structure of turbulence in a boundary layer in the presence of heat transfer. Ph.D. thesis, University of Sydney.

TOWNSEND, A. A. 1965*a* Self-preserving flow inside a turbulent boundary layer. *J. Fluid Mech.* **22**, 773.

TOWNSEND, A. A. 1965*b* The response of a turbulent boundary layer to abrupt changes in surface conditions. *J. Fluid Mech.* **22**, 779.

VEROLLET, E. & FULACHIER, L. 1969 Mesures de densités de flux de chaleur et de tensions de Reynolds dans une couche limite turbulente avec aspiration à la paroi. *C. R. Acad. Sci. Paris*, A **268**, 1577.

WYGNANSKI, I. J. & FIEDLER, H. E. 1970 The two-dimensional mixing region. *J. Fluid Mech.* **41**, 327.

WYNGAARD, J. C. 1971 Spatial resolution of a resistance wire temperature sensor. *Phys. Fluids*, **14**, 2052.